Review

Avant-Garde Polymer and Nano-Graphite-Derived Nanocomposites—Versatility and Implications

Ayesha Kausar [1,2,3]

1 NPU-NCP Joint International Research Center on Advanced Nanomaterials and Defects Engineering, National Centre for Physics, Islamabad 44000, Pakistan; dr.ayeshakausar@yahoo.com
2 iThemba LABS, UNESCO-UNISA Africa Chair in Nanosciences/Nanotechnology, Somerset West 7129, South Africa
3 NPU-NCP Joint International Research Center on Advanced Nanomaterials and Defects Engineering, Northwestern Polytechnical University, Xi'an 710072, China

Abstract: Graphite (stacked graphene layers) has been modified in several ways to enhance its potential properties/utilities. One approach is to convert graphite into a unique 'nano-graphite' form. Nano-graphite consists of few-layered graphene, multi-layered graphene, graphite nanoplatelets, and other graphene aggregates. Graphite can be converted to nano-graphite using physical and chemical methods. Nano-graphite, similar to graphite, has been reinforced in conducting polymers/thermoplastics/rubbery matrices to develop high-performance nanocomposites. Nano-graphite and polymer/nano-graphite nanomaterials have characteristics that are advantageous over those of pristine graphitic materials. This review basically highlights the essential features, design versatilities, and applications of polymer/nano-graphite nanocomposites in solar cells, electromagnetic shielding, and electronic devices.

Keywords: polymer; nano-graphite; nanocomposite; solar cell; electronics

1. Introduction

Natural graphite has stimulated dynamic research interest towards hybrid polymeric materials [1]. Various polymeric matrices have been characteristically reinforced by graphite filler: polyaniline/graphite, epoxy/graphite, polystyrene graphite, PMMA/graphite, and many others [2]. The inclusion of graphite in polymers has remarkably improved their electrical, thermal, mechanical, and other essential physical properties [3–5]. Pristine graphite- and polymer-based materials have been applied in electronics and energy devices, packaging, anticorrosion coatings, membranes, etc. [6]. However, the stacked layered structure of graphite has limited dispersion in polymers and ensuing final high performance. In this regard, various research attempts have focused on the altered forms of compact graphite structures.

Nano-graphite is an exceptional modified form of graphite, having a mixture of layered graphene, nanosheets, and nanoplatelet components [7]. Nano-graphite has been obtained from pristine graphite by using simple techniques, ranging from physical grinding and sonication to chemical conversion techniques. Similar to graphite, it has been reinforced in polymeric matrices in order to form polymer/nano-graphite nanocomposites [8,9]. However, the properties of the resulting nanocomposites have been found to be better than those of pristine-derived polymeric composites. In particular, nano-graphite has been suggested to possess enhanced dispersion in various polymeric matrices, matrix–nanofiller interactions, and end properties. The recent literature has shown the upgraded utility of nano-graphite-derived nanocomposites in technical application areas, including electronics, EMI, and solar cells [10]. However, no review article has been published in the literature to date regarding high-performance polymer/nano-graphite nanocomposites. Hence, this state-of-the-art review definitely contributes important knowledge towards the

future design possibilities and methodological potential of novel polymer/nano-graphite nanocomposites.

2. Nano-Graphite

Graphite is a naturally abundant carbon allotrope [11]. It is made up of stacked layers of sp^2-hybridized carbon atoms, also known as graphene [12]. The graphene layers are usually held together through weak van der Waals forces. The parallel stacking of carbon layers may form a three-dimensional lattice structure.

Nano-graphite is a simply modified form of graphite. The structure of nano-graphite is actually a mixture of nanocarbon nanomaterials with graphitic nanoplatelets or nanosheets and layered graphene [13]. In nano-graphite, the few-layered graphene may consist of two to ten layers or nanosheets. Moreover, graphene nanoplatelets and few-layered graphite oxides also exist. The nanoplatelets may have a thickness of 30–50 graphene layers. Figure 1 displays a simple illustration of the nano-graphite structure. Nano-graphite has fascinating physicochemical characteristics. The electrical, thermal, and mechanical properties of nano-graphite have been found in between the graphite and graphene layers [14]. The preparation of nano-graphite from graphite has been performed through numerous straight-forward approaches, such as mechanical exfoliation (cavitation [15], shear mixing [16], grinding [17], high-pressure homogenization [18], and microfluidization [19]) and son-ication, as well as various thermal and chemical reduction methods. The mechanical exfoliation methods are preferred for the conversion of graphite to nano-graphite due to their low-cost, no use of toxic chemicals, and environmental friendliness [20]. Blomquist and co-workers [21] applied a metal-free aqueous method to obtain nano-graphite. The detonation technique, involving the use of oxygen-deficient explosives, has also been adopted to form nano-graphite [22]. Ioni et al. [23] applied high-power sonication as a single-step method to attain nano-graphite dispersion in various solvents. In another study, transmission electron microscopy, scanning electron microscopy, atomic force microscopy, X-ray diffraction, and Raman spectroscopy were used to examine the nano-graphite nanos-tructure. The nano-graphite had 30–50 graphene layers in its structure [24]. The lateral sizes of the nano-graphite platelets were found to be in the range of 300–500 nm. The thicknesses of the nano-graphite platelets were ~20–40 nm.
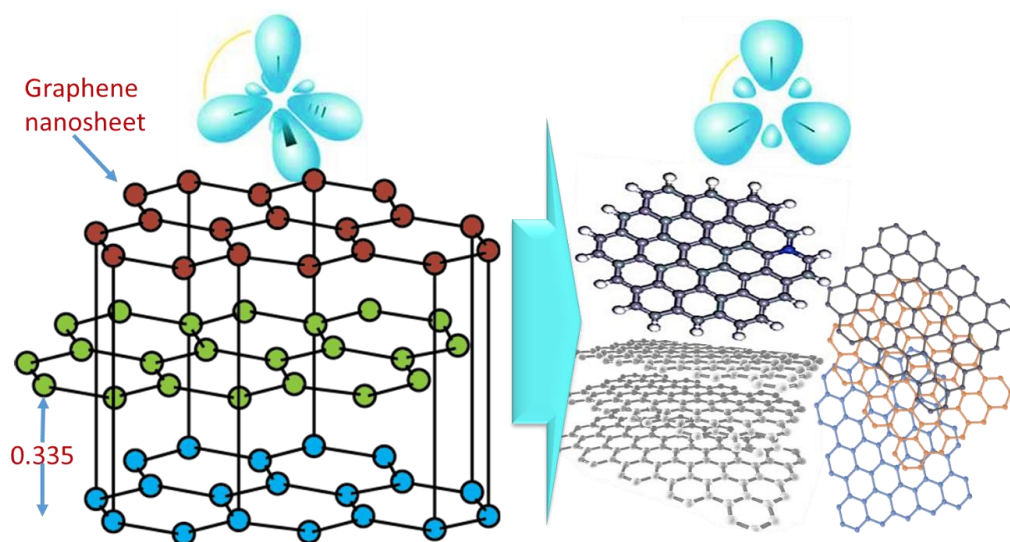

Figure 1. Nano-graphite.

Due to its unique nanostructure, the charge transference properties of nano-graphite have been found to be remarkably high, so it is useful for various related technical applica-tions [25]. The applications of nano-graphite have been observed in thermal/electrical con-ductors, microwave absorbents, lubricants, coatings, absorbents, electromagnetic shields,

gaskets, etc. In polymers, graphite has been applied as an electrically conducting and strengthening filler.

## 3. Polymer and Nano-Graphite-Derived Nanocomposites: Variations and Features

In bulk form, graphite is a layered material with a high electrical conductivity of ~10^6 S/m [26]. Graphite has been widely used as a filler in polymeric composites to improve their electrical, thermal, mechanical, and other physical properties. Polymer/graphite nanocomposites have been fabricated using facile approaches, such as in situ polymerization, solution blending, and melt processing [27]. The graphite dispersion in polymers depends on the choice of the processing technique [28]. It has been observed that graphite particles may develop an interconnecting network to support the percolation threshold of conductivity in the matrix. Nylon 6, polyamides, polystyrene, and other thermoplastics have been effectively filled with graphite using solution mixing in situ and melt routes. The fine graphite content and dispersion have led to the application of polymer/graphite composites in wide a range of applications, from automobile parts to electronics [29].

The performance of polymer/nano-graphite nanocomposites depends on the manufacturing techniques used and the related processing parameters [30]. Polymer/nano-graphite nanocomposites have been mostly processed using solution, melt, in situ, and other facile manufacturing techniques. The choice of technique determines the nanofiller dispersion, matrix–nanofiller interactions, and interface formation, affecting the enhancements in the final material properties [31]. Most importantly, the preparation method and the parameters determine the extent of nanofiller scattering in the polymers. Solution blending has the advantages of fine nanofiller dispersion and the homogeneous morphology of the nanocomposites; however, its major disadvantage is the use of toxic organic solvents [32]. The melt processing system can be considered ecofriendly; however, it may have a nanofiller aggregation problem [33]. The in situ technique has also been successfully used to form polymer/nano-graphite nanocomposites, and it can use eco-friendly solvents [34]. Therefore, the processing of polymer/nano-graphite nanocomposites by using an appropriate manufacturing strategy may form homogeneous microstructures with enhanced electrical, mechanical, thermal, and other physical properties [35].

3.1. Conducting Polymer/Nano-Graphite

Similar to graphite, the reinforcement behavior and features of nano-graphite have been investigated in nanocomposites. Consequently, nano-graphite has been filled in various polymers using suitable processing techniques, such as solution mixing, melt blending, and in situ polymerization [36]. Conducting polymers and graphite-based nanocomposites have been reported [37]. Most importantly, graphite has been frequently used to enhance the electrical conductivity of conjugated polymers [38]. Singhal et al. [39] designed a poly(3,4-ethylenedioxythiophene): poly(styrenesulfonate)- and nano-graphite-based nanocomposite using the solution method. To consistently disperse the nano-graphite, the swift heavy ion method was used with a Ni ion beam of 80 MeV. The swift heavy ion method actually breaks the nano-graphite accumulation due to van der Waals interactions. Figure 2 depicts the solution processing of the poly(3,4-ethylenedioxythiophene): poly(styrenesulfonate)/nano-graphite nanocomposite. After solution processing, the nanocomposite films were cast on a glass substrate through solution evaporation. Figure 3 displays the transmission electron microscopy images of the pristine nano-graphite and the nanocomposite. A cross-section image of the poly(3,4-ethylenedioxythiophene): poly(styrenesulfonate)/nano-graphite nanocomposite after irradiation showed that the nano-graphite stack had 7–8 graphene layers with a 2.6 nm thickness. Moreover, the nano-graphite had an inter-layer distance of 0.335 nm. Shinde and co-workers [40] prepared nano-graphite via planetary ball milling. Then, the polyaniline/nano-graphite nanocomposites were shaped in the form of pellets via cold pressing. The nanocomposites were characterized for their electrical conductivity and hardness. Mo et al. [41] sonicated expanded graphite in a 95% alcohol solution to obtain nano-graphite. Polypyrrole/nano-graphite nanocomposites were developed through in

situ polymerization. The electrical conductivity of the polypyrrole/nano-graphite nanocomposites was enhanced with the nanofiller loading. The maximum electrical conductivity of 80.0 Scm^{-1} was achieved with a 3 wt.% nanofiller. Accordingly, the electrical conductivity of the conducting polymers was further boosted with graphite filler loading.
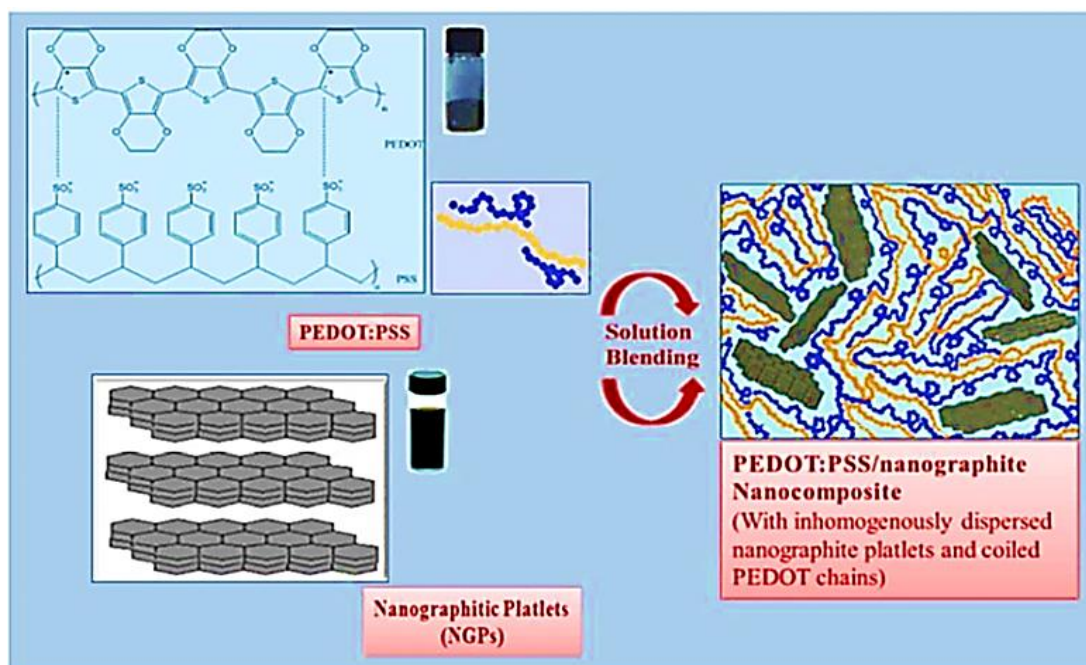
Figure 2. Schematic of poly(3,4-ethylenedioxythiophene):poly(styrenesulfonate)/nano-graphite nanocomposite formation using solution blending technique [39]. Reproduced with permission from ACS.
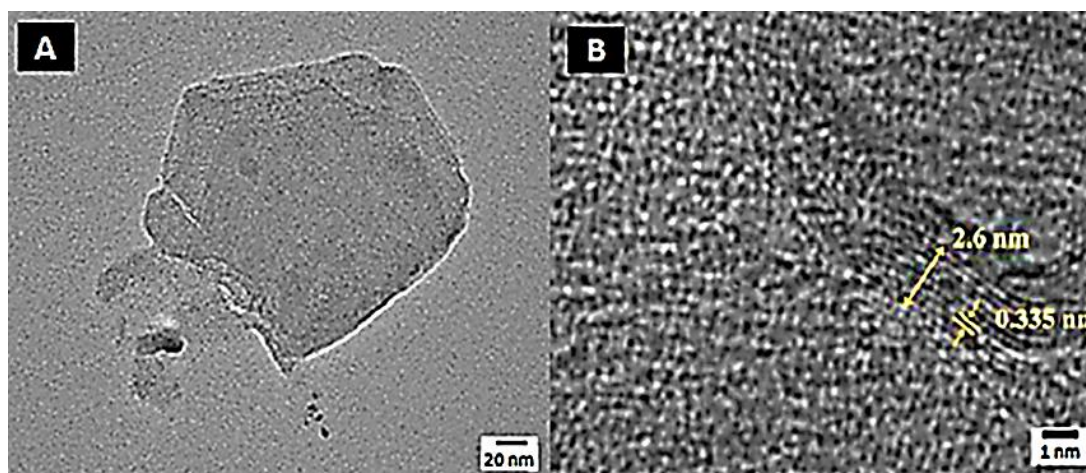

Figure 3. Transmission electron microscopy images of irradiated poly(3,4-ethylenedioxythiophene): poly(styrenesulfonate)/nano-graphite nanocomposite: (**A**) nano-graphite and (**B**) cross-section of nanocomposite showing 2.6 nm-thick nano-graphite stack with characteristic 0.34 nm inter-laminar spacing [39]. Reproduced with permission from ACS.

3.2. Polystyrene/Nano-Graphite

Polystyrene has been widely used as an important matrix for pristine graphite, similarly used with nano-graphite [42–44]. Xuemei et al. [45] adopted the detonation method to form nano-graphite. A nanoparticle size of 16 nm and a specific surface area of 583.6 $\text{m}^2 \cdot \text{g}^{-1}$ were attained by using the Brunauer–Emmett–Teller (BET) equation. The polystyrene/nano-

graphite nanocomposite was prepared via Pickering emulsion polymerization, with azo-bisisobutylonitrile as the initiator in an aqueous solution. Figure 4 displays the optical micrographs of the polystyrene/nano-graphite Pickering emulsion microspheres. The micrographs clearly indicate that the polystyrene microspheres were homogeneously surrounded with a layer of detonation nano-graphite particles. The resulting polystyrene microspheres had a fine dispersity, spherical shape, and uniform size of up to 100 μm. The nanocomposite-encapsulated polystyrene microspheres were polydispersive due to the sonication emulsification method used. A large number of nano-graphite particles densely anchored to form shells around the polystyrene droplets. The use of nano-graphite instead of graphite led to the recompences of better interactions between the nanofiller particles and the polymeric microspheres. The better matrix–nanofiller association and interface formation directly influenced the nano-graphite dispersion and final physical property improvement of the nanocomposite.
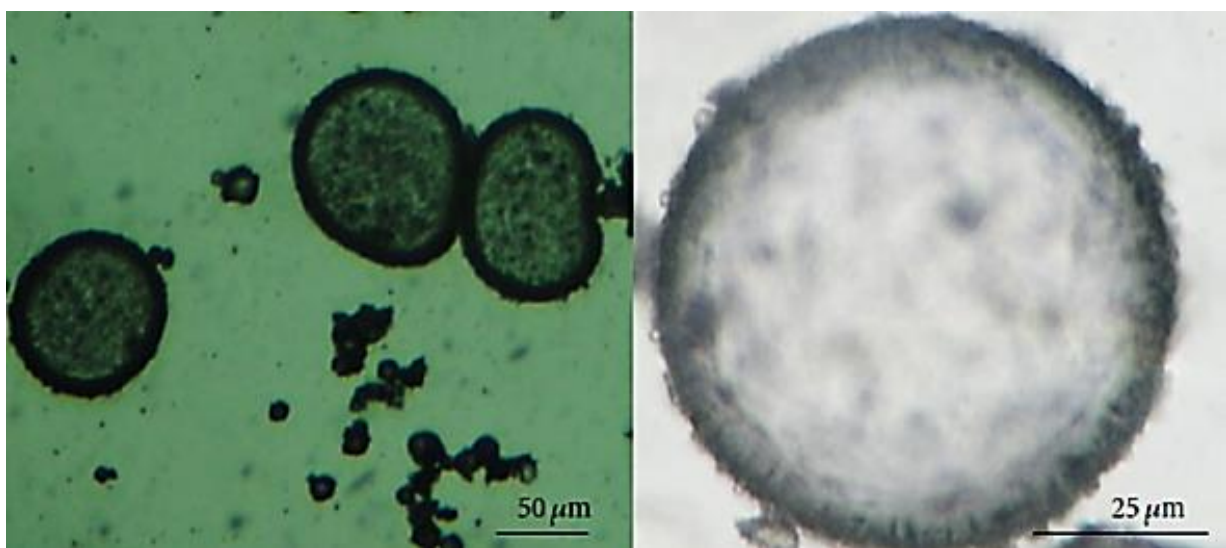
Figure 4. Optical picture of droplet of styrene-in-water Pickering emulsion stabilized by detonation nano-graphite particles [45]. Reproduced with permission from Hindawi.

3.3. Poly(Methyl Methacrylate)/Nano-Graphite

Poly(methyl methacrylate) has been applied as a vital thermoplastic matrix to form nanocomposites with neat graphite [46–48]. Likewise, nano-graphite nanofiller has also been reinforced in poly(methyl methacrylate) matrices. Singhi et al. [49] used commercially obtained nano-graphite of ~400 nm. A poly(methyl methacrylate)/nano-graphite nanocomposite was formed using the in situ polymerization of methylmethacrylate monomer and nano-graphite along with sonication. The nano-graphite was loaded in the range of 0.25–1.5 wt.%. The thermal stability of the neat poly(methyl methacrylate) and poly(methyl methacrylate)/nano-graphite nanocomposites was determined by conducting a thermo-gravimetric analysis (TGA) and differential scanning calorimetry (DSC). The results of the thermal studies are given in Table 1. According to TGA, the initial decomposition temperature of the poly(methyl methacrylate)/nano-graphite nanocomposites increased with the nanofiller loading up to 154 °C relative to that of the neat polymer (114 °C). The DSC thermograms also revealed improvements in the glass transition temperature of up to 114 °C compared with that of the neat polymer (110 °C). The increase in the thermal constancy and glass transition of the nanocomposite can be attributed to the polymer chain stiffness and stability due to the addition of the nano-graphite nanofiller. Soni et al. [50] produced a poly(methyl methacrylate)/nano-graphite nanocomposite by using the solution casting technique. The nano-graphite nanofiller was loaded in 1–5 wt.% contents. The nanocomposite was studied for its optical properties. The optical properties of the poly(methyl methacrylate)/nano-graphite nanocomposite were not affected by the nanofiller loading;

however, the optical properties of the films decreased with an increase in the temperature. The reason for this seems to be the decrease in the transmittance and energy bandgap at higher temperatures. Poly(methyl methacrylate)/nano-graphite nanocomposites have been fabricated through in situ and solution methods. The effect of nano-graphite loading has mostly been considered for the enhancement of optical and thermal properties.

Table 1. Results of thermal characterization of poly(methyl methacrylate)/nano-graphite nanocomposite [49]. Reproduced with permission from Wiley.

Nano-Graphite (wt.%)	Glass Transition Temperature (°C)	Initial Thermal Decomposition Temperature (°C)
Neat	110.6	114.5
0.25	107.8	97.72
0.50	112.1	153.9
0.75	116.6	132.5
1.0	112.0	126.2
1.5	–	88.67

3.4. Poly(Vinyl Chloride)/Nano-Graphite

Poly(vinyl chloride)- and graphite-based materials have gained considerable research interest [51–53]. Poly(vinyl chloride) is another thermoplastic matrix nanocomposite with nano-graphite. Zhang et al. [54] adopted commercial nano-graphite to form a nanocomposite with a titania and poly(vinyl chloride) matrix. The photocatalytic degradation mechanism of the poly(vinyl chloride) nanocomposite with nano-graphite and titania is demonstrated in Figure 5. The nano-graphite and titania were consistently distributed in the polymeric matrix and, thus, improved the conductivity and photocatalytic activity of the nanomaterial. Figure 6 shows that the photocatalytic degradation weight loss of the nanocomposite was significantly more enhanced than that of the neat poly(vinyl chloride) and pristine nano-graphite. The inclusion of the combination of nanocarbon and titania not only upsurged the photocatalytic efficiency due to electron/photon transfer but also promoted structural stability due to interfacial interactions. Although few poly(vinyl chloride)/nano-graphite systems have been explored to date, enhancements in dispersion, thermal, and photocatalytic behaviors have been observed with nanofiller loading.
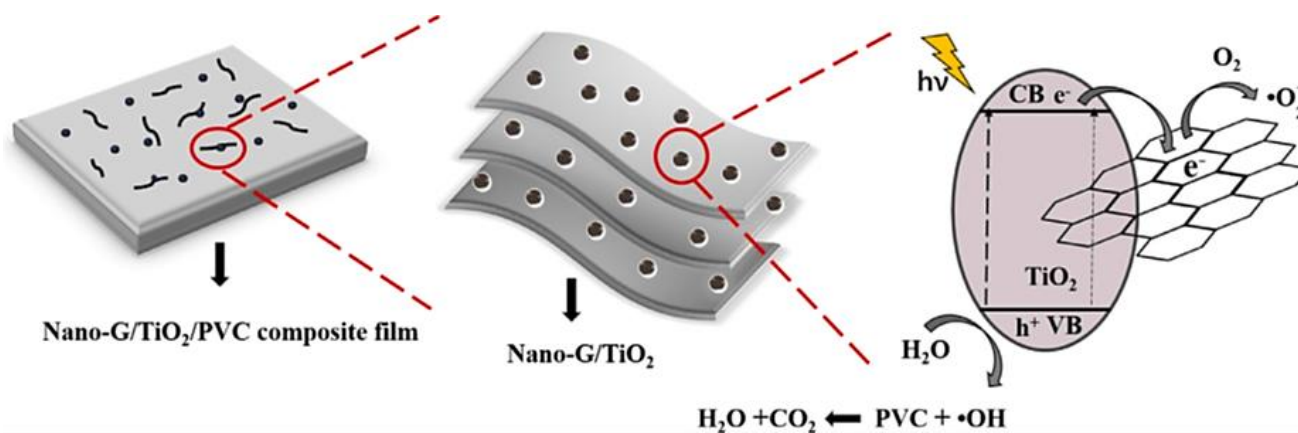
Figure 5. The photocatalytic degradation mechanism of the nanocomposite. Nano-G = nano-graphite; PVC = poly(vinyl chloride); Nano-G/TiO$_2$/PVC = nano-graphite/titania/poly(vinyl chloride) [54]. Reproduced with permission from Elsevier.
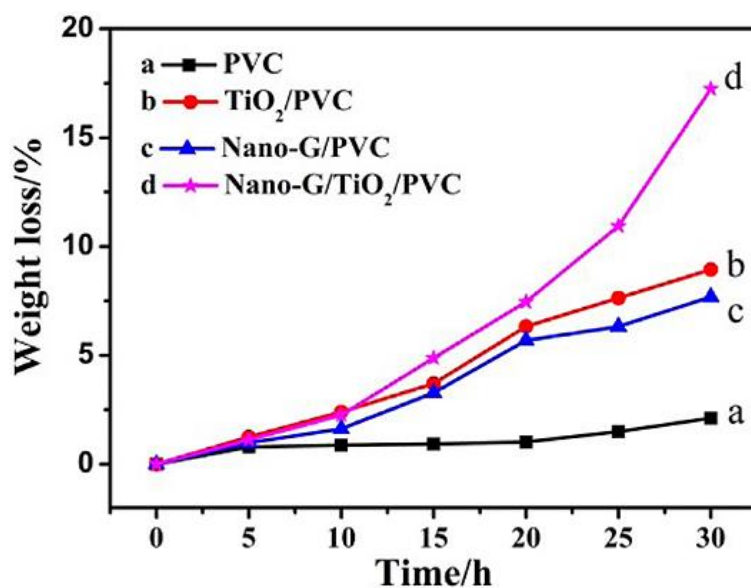
Figure 6. Photocatalytic degradation weight loss curves: (a) poly(vinyl chloride) (PVC); (b) titania/poly(vinyl chloride) (TiO$_2$/PVC); (c) nano-graphite/poly(vinyl chloride) (Nano-G/PVC); (d) nano-graphite/titania/poly(vinyl chloride) (Nano-G/TiO$_2$/PVC) [54]. Reproduced with permission from Elsevier.

3.5. Poly(Vinylidene Fluoride)/Nano-Graphite

Into the bargain, the literature reports on poly(vinylidene fluoride)- and graphite-based materials were examined [55–57]. Poly(vinylidene fluoride) has also been adopted to form a nanocomposite with a nano-graphite nanofiller. Li et al. [58] developed nanocomposites of poly(vinylidene fluoride) and nano-graphite via solution casting and compression molding. The nanofiller contents at the percolation threshold were efficient in improving the dielectric permittivity of the nanocomposite. Abdelaziz et al. [59] reported the development of a poly(vinylidene fluoride)-, hydroxypropyl cellulose-, and nano-graphite-based nanocomposite via the solution method. The addition of nano-graphite generated the β-phase polymorph in the poly(vinylidene fluoride) and matrix–nanofiller interface. Due to the β-phase and interface effects, the dielectric and thermal properties of the nanocomposite were positively affected. Again, in the case of the poly(vinylidene fluoride)/nano-graphite nanocomposite, the literature is limited. Further efforts are required in order to uncover the features and technical potential of poly(vinylidene fluoride)/nano-graphite nanocomposites.

3.6. Poly(Lactic Acid)/Nano-Graphite

The literature also reports poly(lactic acid)- and graphite-derived composites [60–62]. Correspondingly, research has led to the inclusion of nano-graphite in poly(lactic acid) nanocomposites. Gardella et al. [63] produced nano-graphite through the sonication of graphite in an ionic liquid, 1-butyl-3-methylimidazoliumhexa-fluorophosphate (80 °C). The ionic liquid was also used as a medium to disperse the nano-graphite in order to form a nanocomposite with poly(lactic acid). The poly(lactic acid)/nano-graphite nanocomposite was processed via melt blending. The ionic liquid solvent was stable and did not decompose during the nanocomposite processing. According to a scanning electron microscopy analysis, nano-graphite aggregates of 300 nm were observed in the matrix. Guo et al. [64] used a commercial nano-graphite with a diameter of 1.5–2.0 μm. Poly(lactic acid)/nano-graphite nanocomposites were designed via Fused Deposition Modeling. Figure 7 shows the thermal conductivity of the poly(lactic acid)/nano-graphite nanocomposites with varying nanofiller contents. The thermal conductivity increased with an increase in the nano-graphite content. The reason for this was the formation of transportation conducting pathways due to the nanofiller linking in the polymeric matrices. Owing to the high thermal/electrical con-

ductivity, the poly(lactic acid)/nano-graphite nanocomposites were printed using Fused Deposition Modeling. Figure 8 shows the printed models on paper and flexible materials. The printed models had a fine flexibility and adhesion to the substrates due to fine matrix–nanofiller interactions and interface formation.
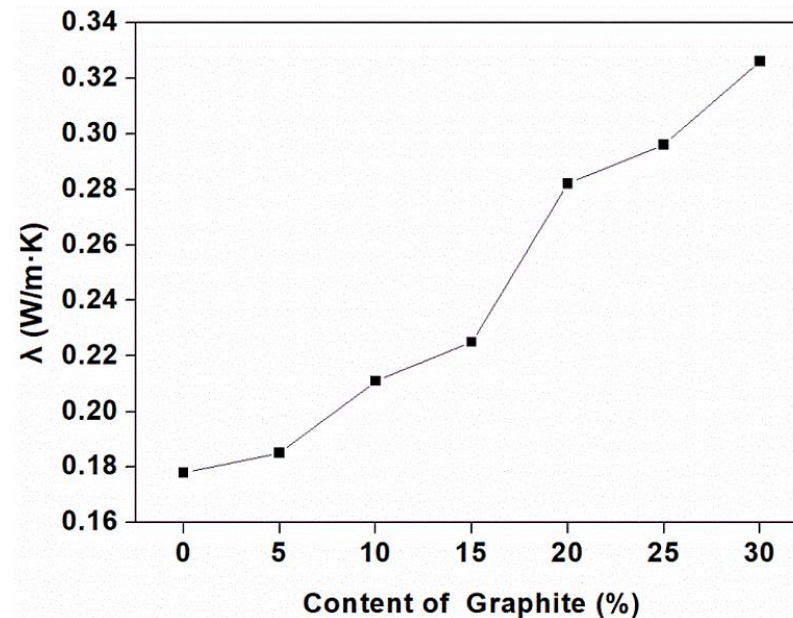
Figure 7. Thermal conductivity of poly(lactic acid)/nano-graphite nanocomposites with different nano-graphite loadings [64]. Reproduced with permission from MDPI.
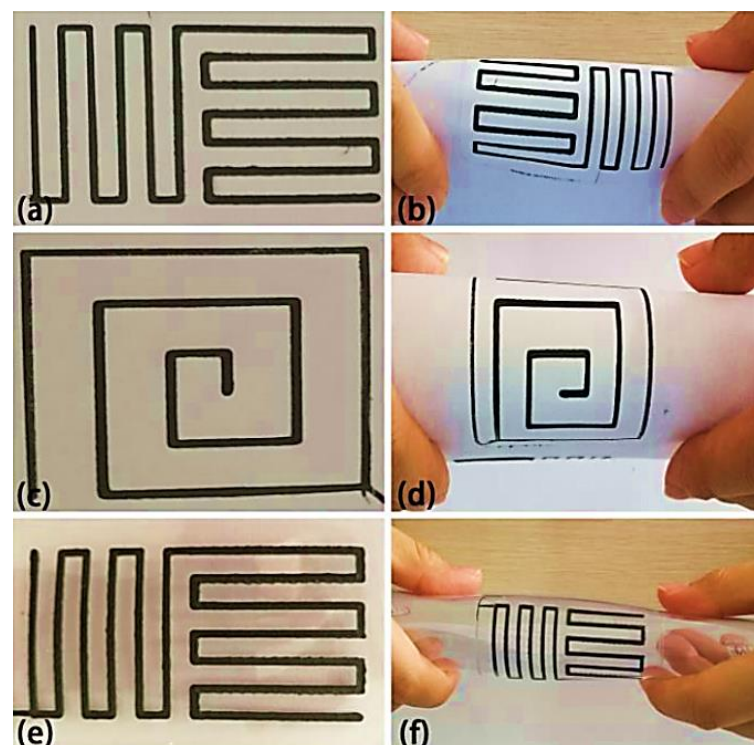
Figure 8. Models printed via Fused Deposition Modeling on different baseplates: (**a**,**c**) different shapes printed on paper; (**b**,**d**) the bend parts; (**e**) models printed on flexible materials; and (**f**) the bend parts [64]. Reproduced with permission from MDPI.

3.7. Polyurethane/Nano-Graphite

Polyurethane has also been applied as an important nanocomposite matrix. Mishra et al. [65] developed a polyurethane/nano-graphite nanocomposite for energy devices. The electrical conductivity of the polyurethane/nano-graphite nanocomposite with varying nanofiller contents is shown in Figure 9.
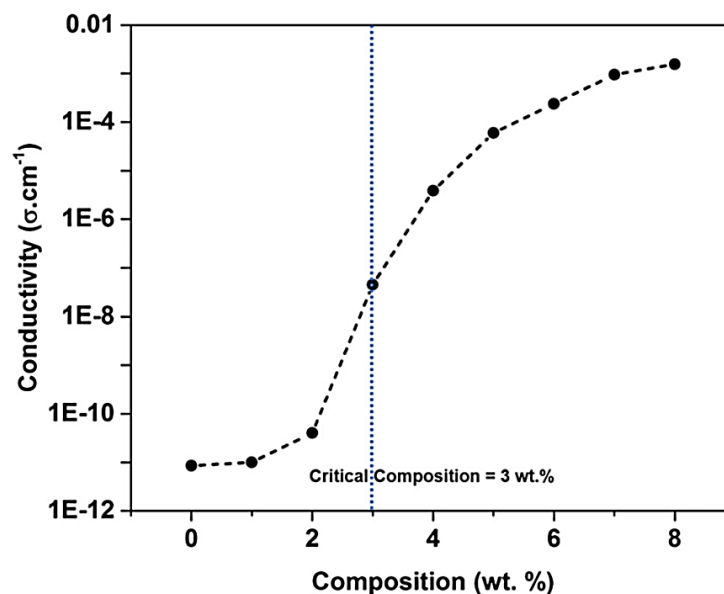
Figure 9. Variation in electrical conductivity of polyurethane/nano-graphite nanocomposite with varying nanofiller contents [65]. Reproduced with permission from Springer.

The percolation threshold of the nano-graphite in the polyurethane matrix was analyzed. The electrical conductivity of the polyurethane/nano-graphite nanocomposite was enhanced after the addition of 3 wt.% nanofiller, and it was stabilized after 5 wt.%. The 3 wt.% nano-graphite content was used as the percolation threshold value for energy device applications. Although there have been limited attempts to develop polyurethane/nano-graphite nanocomposites, the effect of the nanofiller on the conductivity properties points to the important technical significance of these nanomaterials.

3.8. Rubber/Nano-Graphite

Rubber- and graphite-based composites have gained vital importance due to their thermal/mechanical properties and engineering applications [66,67]. El-Nashar et al. [68] prepared nano-graphite using a poly(ethylene glycol)-based method. In acrylonitrilebutadiene rubber, the nano-graphite nanoparticles enhanced the mechanical properties (Young's modulus and hardness) and thermal stability of the matrix. According to dielectric studies, the permittivity and dielectric loss were found to increase with a rapid increase in the percolation threshold upon the addition of the nano-graphite. The acrylonitrilebutadiene rubber/nano-graphite nanocomposite was found to be useful for antistatic applications. Tiwari et al. [69] loaded nano-graphite in a chlorobutyl elastomer matrix. A nano-graphite loading of 6 phr was used as the percolation threshold in order to enhance the electrical conductivity of the nanocomposite. Scanning electron microscopy revealed some agglomerative nano-graphite nanoparticles, as well as the formation of an unremitting network in the matrix. The storage modulus and dielectric properties of the rubber/nano-graphite nanocomposite were dependent on the matrix–nanofiller interactions and were also affected by the rubber–nano-graphite network formation. Thus, rubber/nano-graphite nanocomposites have been investigated due to their advantageous dispersion, conductivity, dielectric, thermal, and mechanical features for relevant practical applications.

Hence, various polymers, such as poly(3,4-ethylenedioxythiophene): poly(styrenesulfonate), polyaniline, polypyrrole, polystyrene, poly(methyl methacrylate), poly(vinyl chloride), poly(vinylidene fluoride), poly(lactic acid), polyurethane, acrylonitrilebutadiene rubber, chlorobutyl elastomer, and silicone rubber, have been employed as matrices for nano-graphite nanofillers. The dispersion of the nanofiller in the conducting polymer matrices formed via in situ methods have been found to be superior. Moreover, the nanofiller dispersion in thermoplastic matrices via solution methods has also been found to be homogeneous. All the conducting polymers, thermoplastics, and rubbery matrices behave differently with nano-graphite in terms of physical properties, depending on the backbone composition. Hence, advantageous properties can be obtained using various polymers and nano-graphite nanofillers, and no single polymer/nano-graphite nanocomposite category can be referred to as the best. However, nanofiller dispersion has been found to be dependent on the amount of nanofiller loaded, as well as on the processing technique used for the nanocomposite formation. The fine nanofiller dispersion attained via the facile processing technique may lead to enhanced properties for all the polymer/nano-graphite categories.

The structure of the nano-graphite affects the final properties and performance of the nanocomposites. Therefore, nano-graphite with a fine quality, the least impurities, and less structural disorders plays an essential role in the improvement of nanofiller dispersion, the provision of superior physical properties, and the production of high-performance nanocomposites. Consequently, the addition of nano-graphite influences the microstructure, surface morphology, and phase composition of nanocomposites. Subsequently, nano-graphite affects the compatibility of the polymer–nanofiller in a nanomaterial. In particular, the thermal stability, glass transition temperature, thermal conductivity, electrical conductivity, and mechanical behavior have been tuned with the addition of nano-graphite nanofiller. The better nano-graphite interactions with the polymer chains lead to mechanical interlocking, which enhances the mechanical properties. Moreover, the polymer chain rigidity and stability improve, leading to an upgraded heat stability and glass transition temperature. The inclusion of nanofiller in polymers through physical/covalent means also affects electron and thermal transportation through the nanocomposite systems.

## 4. Application Arenas of High-Performance Polymer/Nano-Graphite Nanocomposites

4.1. In Dye-Sensitized Solar Cells

A dye-sensitized solar cell (DSSC) is usually composed of counter electrodes as crucial components [70]. Platinum (Pt) has been commercially used as a counter electrode in DSSCs in addition to indium tin oxide or fluorine tin oxide electrodes [71]. Pt-electrode-based DSSCs have the disadvantages of a high cost and weight. Pt electrodes have been beneficially replaced with carbon-based materials [72]. For instance, graphite, carbon black, carbon nanotubes, etc., have been used as DSSC electrodes, showing high conductivity [73,74]. To constructively use carbon materials in electrodes, conducting polymers, such as poly(3,4-ethylenedioxythiophene):poly(styrene sulfonate) [75], polyaniline [76], and polypyrrole [77], have been used. Polyaniline-based nanocomposites are frequently fabricated for DSSC electrodes [78]. Polyaniline/graphite nanocomposites have been used in DSSC electrodes [79]. Correspondingly, Huang et al. [80] applied a polyaniline/nano-graphite nanocomposite in a DSSC counter electrode. The polyaniline/nano-graphite nanocomposite was prepared by using electro-polymerization. The power-conversion efficiency of the polyaniline/nano-graphite-nanocomposite-based DSSC was high at ~7.07%, i.e., comparable to the platinum electrode DSSC (7.19%). Yue et al. [81] prepared various counter electrodes for DSSCs, such as polypyrrole (PPy), platinum (Pt), nano-graphite (NG), and nano-graphite/polypyrrole (NG/PPy) counter electrodes. Figure 10 shows the comparative electrochemical impedance spectra (EIS) of the counter electrodes studied. The electrochemical performance of the NG/PPy electrode revealed a low charge-transfer resistance at the electrolyte–electrode interface, as well as excellent electrocatalyst performance. From the EIS spectra, the electrocatalytic activity of NG/PPy was determined from a semicircle diameter to be 0.1–100 kHz. The photovoltaic performance of the DSSC is

given in Figure 11 and Table 2. Among all the electrodes, the DSSC with the NG/PPy electrode had a higher short-circuit current density and a power conversion efficiency of 14.83 mA·cm^{-2} and 7.40%, respectively. In solar cells, more novel polymer/nano-graphite combinations have been found to be desirable to attain a high power conversion efficiency of >8%.
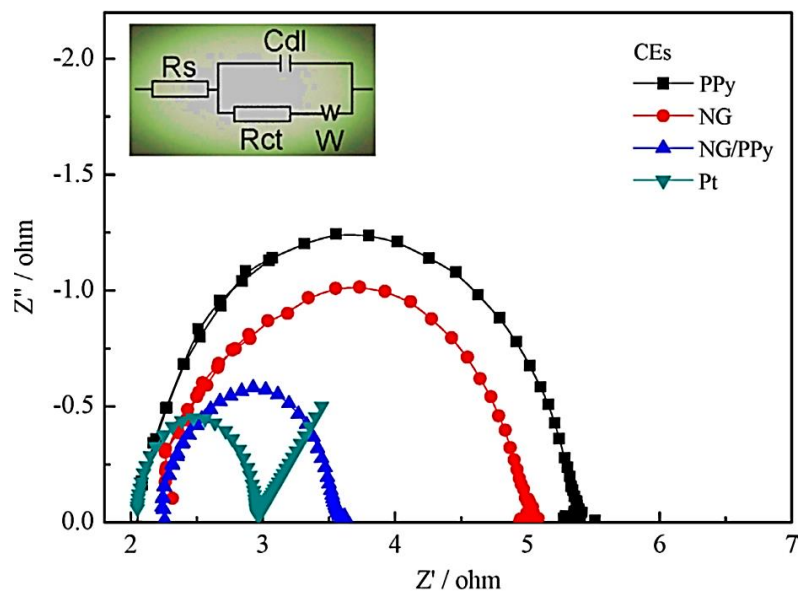
Figure 10. Nyquist plots of counter electrodes (CEs), i.e., graphite/polypyrrole (NG/PPy), polypyrrole (PPy), platinum (Pt), and nano-graphite (NG). Rs = Ohmic serial resistance; Rct = charge-transfer resistance of single electrode; Cdl = double-layer capacitance; W = diffusion impedance [81]. Reproduced with permission from Elsevier.
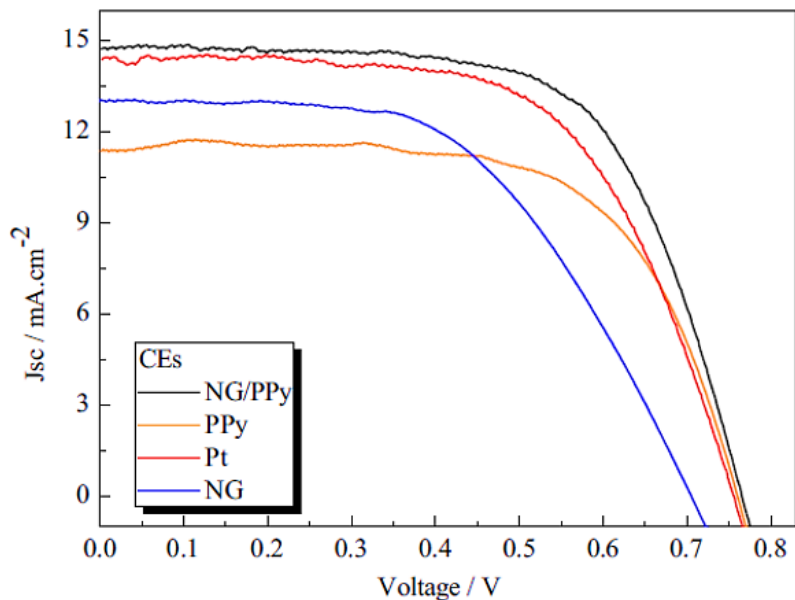

Figure 11. Photocurrent–voltage characteristics of dye-sensitized solar cell with nano-graphite/polypyrrole (NG/PPy)-, polypyrrole (PPy)-, platinum (Pt)-, and nano-graphite (NG)-based counter electrodes (CEs) under illumination of AM 1.5 G [81]. Reproduced with permission from Elsevier.

Table 2. Photocurrent-voltage parameters of dye-sensitized solar cell with nano-graphite/polypyrrole (NG/PPy), polypyrrole (PPy), Platinum (Pt), and nano-graphite (NG) under the illumination of AM 1.5 [81]. Voc = open-circuit voltage; Jsc = short-circuit current densit; FF = fill factor; PCE = power conversion efficiency. Reproduced with permission from Elsevier.

Sample	Voc (v)	Jsc (mA·cm^{-2})	FF	PCE (%)
PPy	0.760	11.74	0.632	5.64
NG	0.705	13.04	0.582	5.35
Pt	0.755	14.54	0.636	6.98
NG/PPy	0.765	14.83	0.652	7.40

4.2. In Electronics

Electronic devices, such as stretchable sensors, actuators, and flexible electrical devices, have been focused on for the use of innovative nanomaterials [82,83]. Polymer- and graphite-derived materials have been applied in next-generation electronic devices [84]. A polytetrafluoroethylene/nano-graphite grid was prepared and compared with a commercial lead alloy (Figure 12). The polytetrafluoroethylene/nano-graphite grid had a smooth surface (Figure 12B,C), and it was more efficiently used as a negative current collector in batteries compared to the commercial lead-based grids (Figure 12A). Room-temperature-vulcanized (RTV) silicone rubber/nano-graphite-based stretchable strain sensors and actuators have been industrialized [85]. Previously, carbon nanotubes have been used in RTV silicone rubber devices to augment their stiffness to some extent [86].
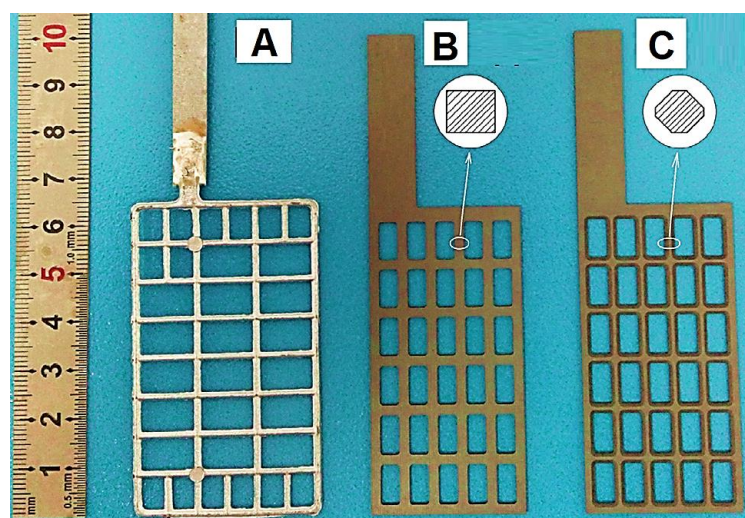

Figure 12. Photographs of (**A**) lead alloy grid and (**B**,**C**) nano-graphite grids with different alignments [84]. Reproduced with permission from Wiley.

Nevertheless, the use of new nano-graphite materials has suitably adjusted the flexibility and stretchability of RTV silicone rubber devices [87]. The noteworthy piezo-resistive strain-sensing and actuation performances of RTV silicone rubber/nano-graphite devices have been experiential. Nano-graphite with a few layers of three-dimensional nanoplatelets with a diameter of 12–15 nm was filled in RTV silicone rubber devices. The addition of 5 phr of nano-graphite boosted the compressive modulus and tensile modulus of the RTV devices by 135% and 125%, respectively [88]. The actuation displacement of the RTV silicone rubber/nano-graphite devices was also improved by 32% via a growing voltage supply from 2 to 8 kV. The strain sensor had a high stretchability of >100% and a durability of up to 5000 cycles [89]. In this field, further design investigations into polymer/nano-graphite nanomaterials have been considered significant to the discovery of important uses in next-generation flexible sensors, actuators, and related electronic devices.

4.3. EMI Shielding

The electromagnetic interference pollution from electronic/telecommunication instruments is continuously affecting human, biological, and environmental systems [90]. Electromagnetic interference (EMI)-shielding materials have been developed to reduce adverse radiation affects [91]. EMI shielding reduces incident radiation via the reflection and absorption phenomenon through a material. Consequently, EMI-shielding materials provide protection against incident radiation. Electrical conductivity has been considered to be an important property of EMI-shielding materials [92]. Initially, metals were applied as EMI shields [93]. However, metallic materials have the disadvantages of a high cost, a heavy weight, corrosion, and processability problems [94]. In this regard, electrically conducting polymeric composites have been used to overawe the limits of metal shields [95]. Carbon fillers have high aspect ratios, permittivity, permeability, and intrinsic conductivity for a high EMI-shielding performance [96]. Accordingly, conducting fillers, such as graphite, carbon black, and carbon nanotubes, have been filled in polymeric matrices to potentially improve EMI shielding [97,98]. Graphite-based materials have been preferably applied in EMI shields [99]. Jeddi and co-researchers [100] developed silicon rubber/nano-graphite nanocomposites and studied their EMI-shielding effectiveness. The nanomaterials had a high electrical conductivity and low percolation threshold values, contributing to radiation protection. According to X-ray band frequency studies, the absorption loss was found to be a leading mechanism for the intensity attenuation of incident electromagnetic waves. In another attempt, Jeddi et al. [101] designed silicon rubber/nano-graphite/carbon black nanocomposites. The nanomaterials had a fine conducting network that promoted electrical properties and, thus, EMI shielding. The dielectric permittivity of the silicon rubber with the nano-graphite, carbon black, and nano-graphite/carbon black is shown in Figure 13. The values of the dielectric permittivity increased with an increase in filler contents. The combination of nano-graphite/carbon black in the silicon rubber was effective in enhancing the dielectric permittivity relative to that of the silicon rubber/nano-graphite nanocomposite. The effect was observed due to the attainment of the percolation threshold and the polarization of the matrix–nanofiller interface. The absorption loss was found to be a major mechanism for the attenuation of incident EMI radiation in these nanocomposites. However, to date, very limited nano-graphite-based design options have been discovered for EMI shields. The development of novel polymer/nano-graphite nanocomposites may result in practically important high-performance radiation-shielding materials.
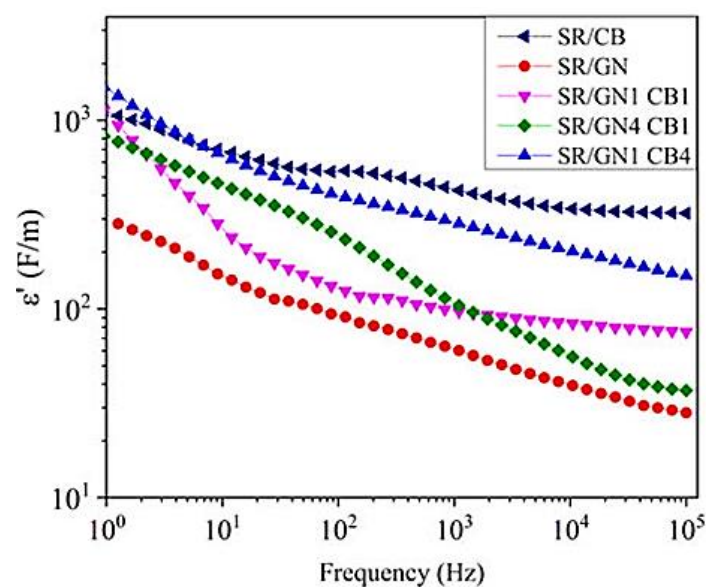
Figure 13. Real permittivity (ε') properties of silicon rubber (SR) nanocomposites with sample nano-graphite (GN) and carbon black (CB) nanofillers [101]. Reproduced with permission from Elsevier.

5. Future Perspectives, Challenges, and Conclusions

Table 3 demonstrates the processing strategies, noteworthy features, and technical applications of polymer/nano-graphite nanocomposites. Nano-graphite nanofiller has been reinforced in polymer matrices to improve structural, morphological, electrical conductivity, thermal conductivity, dielectric characteristics, thermal stability, mechanical properties, photovoltaics, sensing/actuating, radiation shielding, and other physical properties. Nano-graphite nanoparticles have been prepared using various facile physical and chemical methods.

Table 3. Specifications and impact of polymer/nano-graphite nanocomposites.

Polymer	Nanofiller/Preparation Method	Nanocomposite Fabrication	Property/Application	Ref
Poly(3,4-ethylenedioxythiophene): poly(styrenesulfonate)	Nano-graphite; 7–8 graphene layers; 2.6 nm thickness	Solution method	Dispersion; swift heavy ions	[39]
Polyaniline	Nano-graphite; planetary ball milling	Cold pressing	Electrical conductivity; hardness	[40]
Polypyrrole	Nano-graphite; sonication in 95% alcohol solution	In situ polymerization	Electrical conductivity 80.0 Scm^{-1}	[41]
Polystyrene	Nano-graphite; detonation method; size 16 nm; specific surface area 583.6 m$^2 \cdot$g^{-1}	Pickering emulsion	Morphology; polystyrene microspheres encapsulated with nano-graphite shield	[45]
Poly(methyl methacrylate)	Commercial nano-graphite; ~400 nm	In situ polymerization	Thermogravimetric analysis; initial decomposition temperature ~154 °C	[49]
Poly(methyl methacrylate)	Nano-graphite	Solution casting technique	Optical properties; thermal stability	[50]
Poly(vinyl chloride)	Commercial nano-graphite; Titania	Solution casting technique	Conductivity; photocatalytic activity	[54]
Poly(vinylidene fluoride)	Nano-graphite	Solution casting; compression molding	Percolation threshold; dielectric permittivity	[58]
Poly(vinylidene fluoride)	Nano-graphite	Solution method	β-phase; interface effects	[59]
Poly(lactic acid)	Nano-graphite; sonication of graphite in ionic liquid, 1-butyl-3-methylimidazoliumhexa-fluorophosphate	Melt blending	Aggregates of 300 nm	
Poly(lactic acid)	Commercial. nano-graphite; diameter 1.5–2.0 μm	Fused Deposition Modeling	Thermal conductivity; conducting pathways	[64]
Polyurethane	Nano-graphite	Solution method	Percolation threshold; electrical conductivity	[65]
Acrylonitrilebutadiene rubber	Nano-graphite in poly(ethylene glycol)	Melt method	Young's modulus; hardness; thermal stability; permittivity; dielectric loss; antistatic application	[68]

Table 3. *Cont.*

Polymer	Nanofiller/Preparation Method	Nanocomposite Fabrication	Property/Application	Ref
Chlorobutyl elastomer	Nano-graphite	Melt method	Percolation threshold; storage modulus; dielectric properties	[69]
Polyaniline	Nano-graphite	Electro-polymerization	DSSC counter electrode; power-conversion efficiency ~7.07%	[80]
Polypyrrole	Nano-graphite	Electro-polymerization	Electrochemical impedance spectroscopy; power-conversion efficiency ~7.40%	[81]
Room temperature vulcanized silicone rubber	Nano-graphite; 12–15 nm diameter	Melt; solution; printing	Sensors/actuators; piezo-resistive strain sensing; compressive modulus; tensile modulus stretchability >100%; durability of up to 5000 cycles	[86–89]
Silicon rubber	Nano-graphite; carbon black	Melt route	Electromagnetic interference shielding	[100,101]

The future of polymer/nano-graphite nanocomposites relies on their potential applications in various technical fields. The potential application of polymer/nano-graphite nanocomposites has been observed for DSSCs. High-performance solar cells can be achieved due to the geometric and electronic effects of the nano-graphite in the conducting polymers. A high power conversion efficiency can be achieved for these nanocomposites. In future, a higher efficiency can be attained by using functional nano-graphite nanostructures. Nano-graphite-based nanocomposites also possess potential for use in electronics, sensors, and actuator devices. However, future efforts are needed to design high-performance polymer/nano-graphite nanocomposites for commercial electronic device applications. Similarly, the potential application of polymer/nano-graphite nanocomposites has been observed for EMI nanomaterials. Future efforts may lead to a high EMI shielding efficiency of >50 dB for commercial applications. Consequently, due to the restricted research in various fields, several future technical grounds still need to be explored for polymer/nano-graphite nanocomposites. Forthcoming research on these innovative nanomaterials may lead to applications in batteries, aerospace/automobiles, construction materials, and biomedical areas.

Challenges regarding the use of polymer/nano-graphite nanocomposites have been found related to their properties, performance, and structure–property relationship. The nanofiller dispersion has been pointed out as the main challenge in the application of polymer/nano-graphite nanocomposites. The dispersion issues can be overcome by using the appropriate processing technique and controlled processing parameters. Moreover, the use of optimum nanofiller contents and functional nano-graphite may result in better matrix–nanofiller interactions, interface formation, and a homogeneous dispersion in the polymers. In polymer/nano-graphite nanocomposites, the augmentation of the physical property in fact relies on the nano-graphite dispersion in the polymers. Additionally, it is important to understand the mechanisms of physical and chemical interactions and interface formation in polymer/nano-graphite nanocomposites in order to develop high-performance nanomaterials.

Succinctly, this appraisal provides a novel insight into polymer/nano-graphite nanocomposites. Nano-graphite has been found to be practical as a unique nanofiller for polymeric nanocomposites. Numerous facile strategies have been used to design nano-graphite nanoparticles and polymer/nano-graphite nanocomposites. Polymer/nano-graphite nanocomposites have uncovered important structural, morphological, electrical, thermal, mechanical, and other essential properties. The applications of polymer/nano-graphite nanocomposites have been extended to DSSCs, electronics, and EMI-shielding devices. Future research on functional nano-graphite and polymer/nano-graphite nanocomposites may lead to enormous progressions in the related technical fields.

Conflicts of Interest: The authors declare no conflict of interest.

References

1. Morgan, D.J. Comments on the XPS analysis of carbon materials. *C* **2021**, *7*, 51. [CrossRef]
2. de Souza, F.M.; Choi, J.; Bhoyate, S.; Kahol, P.K.; Gupta, R.K. Expendable graphite as an efficient flame-retardant for novel partial bio-based rigid polyurethane foams. *C* **2020**, *6*, 27. [CrossRef]
3. Cazzanelli, M.; Basso, L.; Cestari, C.; Bazzanella, N.; Moser, E.; Orlandi, M.; Piccoli, A.; Miotello, A. Fluorescent Nanodiamonds Synthesized in One-Step by Pulsed Laser Ablation of Graphite in Liquid-Nitrogen. *C* **2021**, *7*, 49. [CrossRef]
4. Odusanya, A.; Rahaman, I.; Sarkar, P.K.; Zkria, A.; Ghosh, K.; Haque, A. Laser-Assisted Growth of Carbon-Based Materials by Chemical Vapor Deposition. *C* **2022**, *8*, 24. [CrossRef]
5. Kausar, A. Poly (methyl methacrylate) nanocomposite reinforced with graphene, graphene oxide, and graphite: A review. *Polym.-Plast. Technol. Mater.* **2019**, *58*, 821–842. [CrossRef]
6. Kausar, A.; Rafique, I.; Muhammad, B. Aerospace application of polymer nanocomposite with carbon nanotube, graphite, graphene oxide, and nanoclay. *Polym.-Plast. Technol. Mater.* **2017**, *56*, 1438–1456. [CrossRef]
7. Blomquist, N.; Koppolu, R.; Dahlström, C.; Toivakka, M.; Olin, H. Influence of substrate in roll-to-roll coated nanographite electrodes for metal-free supercapacitors. *Sci. Rep.* **2020**, *10*, 5282. [CrossRef] [PubMed]
8. Kumar, V.; Forsberg, S.; Engström, A.-C.; Nurmi, M.; Andres, B.; Dahlström, C.; Toivakka, M. Conductive nanographite–nanocellulose coatings on paper. *Flexib. Prin. Electron.* **2017**, *2*, 035002. [CrossRef]
9. Wan, C.; Yao, C.; Li, J.; Duan, H.; Zhan, S.; Jia, D.; Li, Y.; Yang, T. Friction and wear behavior of polyimide matrix composites filled with nanographite. *J. Appl. Polym. Sci.* **2022**, *139*, 52058. [CrossRef]
10. Kumar, V.; Alam, M.N.; Manikkavel, A.; Choi, J.; Lee, D.J. Investigation of silicone rubber composites reinforced with carbon nanotube, nanographite, their hybrid, and applications for flexible devices. *J. Vin. Add. Technol.* **2021**, *27*, 254–263. [CrossRef]
11. Luo, P.; Zheng, C.; He, J.; Tu, X.; Sun, W.; Pan, H.; Zhou, Y.; Rui, X.; Zhang, B.; Huang, K. Structural Engineering in Graphite-Based Metal-Ion Batteries. *Adv. Funct. Mater.* **2022**, *32*, 2107277. [CrossRef]
12. Maier, P.; Xavier Jr, N.F.; Truscott, C.L.; Hansen, T.; Fouquet, P.; Sacchi, M.; Tamtögl, A. How does tuning the van der Waals bonding strength affect adsorbate structure? *Phys. Chem. Chem. Phys.* **2022**, *24*, 29371–29380. [CrossRef] [PubMed]
13. Bianco, A.; Cheng, H.-M.; Enoki, T.; Gogotsi, Y.; Hurt, R.H.; Koratkar, N.; Kyotani, T.; Monthioux, M.; Park, C.R.; Tascon, J.M. All in the graphene family—A recommended nomenclature for two-dimensional carbon materials. *Carbon* **2013**, *65*, 1–6. [CrossRef]
14. Blomquist, N.; Engström, A.-C.; Hummelgård, M.; Andres, B.; Forsberg, S.; Olin, H. Large-scale production of nanographite by tube-shear exfoliation in water. *PLoS ONE* **2016**, *11*, e0154686. [CrossRef] [PubMed]
15. Yi, M.; Li, J.; Shen, Z.; Zhang, X.; Ma, S. Morphology and structure of mono-and few-layer graphene produced by jet cavitation. *Appl. Phys. Lett.* **2011**, *99*, 123112. [CrossRef]
16. Paton, K.R.; Varrla, E.; Backes, C.; Smith, R.J.; Khan, U.; O'Neill, A.; Boland, C.; Lotya, M.; Istrate, O.M.; King, P. Scalable production of large quantities of defect-free few-layer graphene by shear exfoliation in liquids. *Nat. Mater.* **2014**, *13*, 624–630. [CrossRef] [PubMed]
17. Knieke, C.; Berger, A.; Voigt, M.; Taylor, R.N.K.; Röhrl, J.; Peukert, W. Scalable production of graphene sheets by mechanical delamination. *Carbon* **2010**, *48*, 3196–3204. [CrossRef]
18. Nacken, T.; Damm, C.; Walter, J.; Rüger, A.; Peukert, W. Delamination of graphite in a high pressure homogenizer. *RSC Adv.* **2015**, *5*, 57328–57338. [CrossRef]
19. Karagiannidis, P.G.; Hodge, S.A.; Lombardi, L.; Tomarchio, F.; Decorde, N.; Milana, S.; Goykhman, I.; Su, Y.; Mesite, S.V.; Johnstone, D.N. Microfluidization of graphite and formulation of graphene-based conductive inks. *ACS Nano* **2017**, *11*, 2742–2755. [CrossRef]

20. Koppolu, R.; Blomquist, N.; Dahlström, C.; Toivakka, M. High-Throughput Processing of Nanographite–Nanocellulose-Based Electrodes for Flexible Energy Devices. *Ind. Eng. Chem. Res.* **2020**, *59*, 11232–11240. [CrossRef]

21. Blomquist, N.; Wells, T.; Andres, B.; Bäckström, J.; Forsberg, S.; Olin, H. Metal-free supercapacitor with aqueous electrolyte and low-cost carbon materials. *Sci. Rep.* **2017**, *7*, 39836. [CrossRef] [PubMed]

22. Shenderova, O. *Detonation Nanodiamonds: Science and Applications*; CRC Press: Boca Raton, FL, USA, 2014.

23. Ioni, Y.V.; Tkachev, S.; Bulychev, N.; Gubin, S. Preparation of finely dispersed nanographite. *Inorg. Mater.* **2011**, *47*, 597–602. [CrossRef]

24. Chen, Q.; Wang, X.; Wang, Z.; Liu, Y.; You, T. Preparation of water-soluble nanographite and its application in water-based cutting fluid. *Nanoscale Res. Lett.* **2013**, *8*, 52. [CrossRef] [PubMed]

25. Prasad, B.; Sato, H.; Enoki, T.; Hishiyama, Y.; Kaburagi, Y.; Rao, A.; Sumanasekera, G.U.; Eklund, P. Intercalated nanographite: Structure and electronic properties. *Phys. Rev. B* **2001**, *64*, 235407. [CrossRef]

26. Frost, B.R.; Fyfe, W.S.; Tazaki, K.; Chan, T. Grain-boundary graphite in rocks and implications for high electrical conductivity in the lower crust. *Nature* **1989**, *340*, 134–136. [CrossRef]

27. Mokhena, T.C.; Mochane, M.J.; Sefadi, J.S.; Motloung, S.V.; Andala, D.M. *Thermal conductivity of graphite-based polymer composites. Impact of Thermal Conductivity on Energy Technologies*; IntechOpen: London, UK, 2018; Volume 181.

28. Salavagione, H.J.; Martínez, G.; Ellis, G. Recent advances in the covalent modification of graphene with polymers. *Macromol. Rapid Commun.* **2011**, *32*, 1771–1789. [CrossRef]

29. Sadasivuni, K.K.; Ponnamma, D.; Thomas, S.; Grohens, Y. Evolution from graphite to graphene elastomer composites. *Prog. Polym. Sci.* **2014**, *39*, 749–780. [CrossRef]

30. Gorshenev, V. Influence of Technological Conditions in the Formation of Electrically Conductive Thermoplastic Polymer-Graphite Composites. *Inorg. Mater. Appl. Res.* **2022**, *13*, 515–522. [CrossRef]

31. Yan, H.; Tao, X.; Yang, Z.; Li, K.; Yang, H.; Li, A.; Cheng, R. Effects of the oxidation degree of graphene oxide on the adsorption of methylene blue. *J. Hazard. Mater.* **2014**, *268*, 191–198. [CrossRef]

32. Liao, Y.; Cao, L.; Wang, Q.; Li, S.; Lin, Z.; Li, W.; Zhang, P.; Yu, C. Enhanced tribological properties of PEEK-based composite coatings reinforced by PTFE and graphite. *J. Appl. Polym. Sci.* **2022**, *139*, 51878. [CrossRef]

33. Jena, K.K.; AlFantazi, A.; Mayyas, A.T. Efficient and cost-effective hybrid composite materials based on thermoplastic polymer and recycled graphite. *Chem. Eng. J.* **2022**, *430*, 132667. [CrossRef]

34. Jiang, Z.; Liu, X.; Xu, Q.; Zhou, C.; Shang, Y.; Zhang, H. Thermal conductive segregated multi-scale network constructed by ball-milling and in-situ polymerization in PEEK/MWCNT/graphite composite. *Compos. Communicat.* **2022**, *29*, 101035. [CrossRef]

35. Seyedjamali, H.; Pirisedigh, A. Well-dispersed polyimide/TiO2 nanocomposites: In situ sol–gel fabrication and morphological study. *Coll. Polym. Sci.* **2012**, *290*, 653–659. [CrossRef]

36. Psarras, G.C. Nanographite–Polymer Composites. In *Carbon Nanomaterials*; CRC Press: Boca Raton, FL, USA, 2018; pp. 647–673.

37. Radzuan, N.A.M.; Sulong, A.B.; Sahari, J. A review of electrical conductivity models for conductive polymer composite. *Int. J. Hydrog. Energy* **2017**, *42*, 9262–9273. [CrossRef]

38. Krause, P.; Nowoświat, A. Experimental studies involving the impact of solar radiation on the properties of expanded graphite polystyrene. *Energies* **2019**, *13*, 75. [CrossRef]

39. Singhal, P.; Rattan, S. Swift heavy ion irradiation as a tool for homogeneous dispersion of nanographite platelets within the polymer matrices: Toward tailoring the properties of PEDOT: PSS/nanographite nanocomposites. *J. Phys. Chem. B* **2016**, *120*, 3403–3413. [CrossRef]

40. Shinde, H.; Kakani, S.M.; Shinde, S.; More, A.; Kher, J.; Patil, S.R. Mechanically Stable Nano-graphite Polyaniline Composites: Synthesis and Characterization. *Int. J. Innov. Res. Sci. Eng. Technol.* **2014**, *3*, 14164–14171.

41. Mo, Z.L.; Xie, T.-T.; Zhao, Y.-X.; Sun, W.-H.; Guo, R.-B.; He, J.-X. Synthesis of PPy/nano-graphite sheets/TbCl3 composites with high conductivity. *Mater. Manuf. Process.* **2012**, *27*, 1343–1347. [CrossRef]

42. Zhu, Z.-M.; Rao, W.-H.; Kang, A.-H.; Liao, W.; Wang, Y.-Z. Highly effective flame retarded polystyrene by synergistic effects between expandable graphite and aluminum hypophosphite. *Polym. Degrad. Stab.* **2018**, *154*, 1–9. [CrossRef]

43. Han, X.; Cheng, Q.; Bao, F.; Gao, J.; Yang, Y.; Chen, T.; Yan, C.; Ma, R. Synthesis of low-density heat-resisting polystyrene/graphite composite microspheres used as water carrying fracturing proppants. *Polym.-Plast. Technol. Mater.* **2014**, *53*, 1647–1653. [CrossRef]

44. Rymansaib, Z.; Iravani, P.; Emslie, E.; Medvidović-Kosanović, M.; Sak-Bosnar, M.; Verdejo, R.; Marken, F. All-polystyrene 3D-printed electrochemical device with embedded carbon nanofiber-graphite-polystyrene composite conductor. *Electroanalysis* **2016**, *28*, 1517–1523. [CrossRef]

45. Xuemei, H.; Hao, Y. Fabrication of polystyrene/detonation nanographite composite microspheres with the core/shell structure via pickering emulsion polymerization. *J. Nanomater.* **2013**, *2013*, 8. [CrossRef]

46. Soni, G.; Soni, P.; Jangra, P.; Vijay, Y. Optical, mechanical and thermal properties of PMMA/graphite nanocomposite thin films. *Mater. Res. Exp.* **2019**, *6*, 075315. [CrossRef]

47. Ali, E.A.G.E.; Kim, T.; Adhha, M.A. Effects of graphite milling time and composition to tensile properties of poly-methyl methacrylate (PMMA)/graphite composite. *J. Sustain. Sci. Manag.* **2019**, *14*, 4–11.

48. Wang, J.; Shi, S.; Yang, J.; Zhang, W. Multiscale analysis on free vibration of functionally graded graphene reinforced PMMA composite plates. *Appl. Math. Model.* **2021**, *98*, 38–58. [CrossRef]

49. Singhi, M.; Fahim, M. Dielectric properties of nanographite-filled PMMA composites prepared by in situ polymerization. *Polym. Compos.* **2012**, *33*, 675–682. [CrossRef]

50. Soni, G.; Jangir, R.K. Effect of temperature nano graphite doped polymethylmethacrylate (PMMA) composite flexible thin films prepared by solution casting: Synthesis, optical and electrical properties. *Optik* **2021**, *226*, 165915. [CrossRef]

51. Raza, J.; Hamid, A.; Khan, M.; Hussain, F.; Tiehu, L.; Fazil, P.; Zada, A.; Wahab, Z.; Ali, A. Spectroscopic characterization of biosynthesized lead oxide (PbO) nanoparticles and their applications in PVC/graphite-PbO nanocomposites. *Z. Für Phys. Chem.* **2022**, *236*, 619–636. [CrossRef]

52. Focke, W.W.; Muiambo, H.; Mhike, W.; Kruger, H.J.; Ofosu, O. Flexible PVC flame retarded with expandable graphite. *Polym. Degrad. Stab.* **2014**, *100*, 63–69. [CrossRef]

53. Miao, F.; Liu, Y.; Gao, M.; Yu, X.; Xiao, P.; Wang, M.; Wang, S.; Wang, X. Degradation of polyvinyl chloride microplastics via an electro-Fenton-like system with a TiO_2/graphite cathode. *J. Hazard. Mater.* **2020**, *399*, 123023. [CrossRef]

54. Zhang, Y.; Sun, T.; Zhang, D.; Shi, Z.; Zhang, X.; Li, C.; Wang, L.; Song, J.; Lin, Q. Enhanced photodegradability of PVC plastics film by codoping nano-graphite and TiO_2. *Polym. Degrad. Stab.* **2020**, *181*, 109332. [CrossRef]

55. Takahashi, K.; Higa, K.; Mair, S.; Chintapalli, M.; Balsara, N.; Srinivasan, V. Mechanical degradation of graphite/PVDF composite electrodes: A model-experimental study. *J. Electrochem. Soc.* **2015**, *163*, A385. [CrossRef]

56. Iqbal, N.; Lee, S. Mechanical failure analysis of graphite anode particles with PVDF binders in Li-ion batteries. *J. Electrochem. Soc.* **2018**, *165*, A1961. [CrossRef]

57. Li, X.; Wang, X.; Weng, L.; Yu, Y.; Zhang, X.; Liu, L.; Wang, C. Dielectrical properties of graphite nanosheets/PVDF composites regulated by coupling agent. *Mater. Today Commun.* **2019**, *21*, 100705. [CrossRef]

58. Li, Y.; Tjong, S.C.; Li, R. Dielectric properties of binary polyvinylidene fluoride/barium titanate nanocomposites and their nanographite doped hybrids. *eXPRESS Polym. Lett.* **2011**, *5*, 526–534. [CrossRef]

59. Abdelaziz, M.; Abdelrazek, E. The effect of nanographite addition on the physical properties of poly (vinylidene fluoride)/hydroxypropyl cellulose blend. *J. Mater. Sci. Mater. Electron.* **2014**, *25*, 5481–5490. [CrossRef]

60. Wang, G.; Zhao, G.; Wang, S.; Zhang, L.; Park, C.B. Injection-molded microcellular PLA/graphite nanocomposites with dramatically enhanced mechanical and electrical properties for ultra-efficient EMI shielding applications. *J. Mater. Chem. C* **2018**, *6*, 6847–6859. [CrossRef]

61. Przekop, R.E.; Kujawa, M.; Pawlak, W.; Dobrosielska, M.; Sztorch, B.; Wieleba, W. Graphite modified polylactide (PLA) for 3D printed (FDM/FFF) sliding elements. *Polymers* **2020**, *12*, 1250. [CrossRef]

62. Kjelgård, K.G.; Wisland, D.T.; Lande, T.S. 3D printed wideband microwave absorbers using composite graphite/PLA filament. In Proceedings of the 2018 48th European Microwave Conference, Madrid, Spain, 23–27 September 2018; IEEE: Piscataway, NJ, USA, 2018; pp. 859–862.

63. Gardella, L.; Furfaro, D.; Galimberti, M.; Monticelli, O. On the development of a facile approach based on the use of ionic liquids: Preparation of PLLA (sc-PLA)/high surface area nano-graphite systems. *Green Chem.* **2015**, *17*, 4082–4088. [CrossRef]

64. Guo, R.; Ren, Z.; Bi, H.; Xu, M.; Cai, L. Electrical and thermal conductivity of polylactic acid (PLA)-based biocomposites by incorporation of nano-graphite fabricated with fused deposition modeling. *Polymers* **2019**, *11*, 549. [CrossRef]

65. Mishra, P.; Bhat, B.R.; Bhattacharya, B.; Mehra, R. Synthesis and Characterization of High-Dielectric-Constant Nanographite–Polyurethane Composite. *JOM* **2018**, *70*, 1302–1306. [CrossRef]

66. ElFaham, M.M.; Alnozahy, A.M.; Ashmawy, A. Comparative study of LIBS and mechanically evaluated hardness of graphite/rubber composites. *Mater. Chem. Phys.* **2018**, *207*, 30–35. [CrossRef]

67. Aguilar-Bolados, H.; Brasero, J.; López-Manchado, M.A.; Yazdani-Pedram, M. High performance natural rubber/thermally reduced graphite oxide nanocomposites by latex technology. *Compos. Part B Eng.* **2014**, *67*, 449–454. [CrossRef]

68. El-Nashar, D.E.; Rozik, N.N.; Abd El-Messieh, S.L. Mechanical and electrical properties of acrylonitrile-butadiene rubber filled with treated nanographite. *Polimery* **2014**, *59*, 834–844. [CrossRef]

69. Tiwari, S.K.; Choudhary, R.N.P.; Mahapatra, S.P. Dynamic mechanical and dielectric relaxation studies of chlorobutyl elastomer nanocomposites: Effect of nanographite loading and temperature. *High Perform. Polym.* **2015**, *27*, 274–287. [CrossRef]

70. Nazeeruddin, M.K.; Baranoff, E.; Grätzel, M. Dye-sensitized solar cells: A brief overview. *Solar Energy* **2011**, *85*, 1172–1178. [CrossRef]

71. Yun, S.; Hagfeldt, A.; Ma, T. Pt-free counter electrode for dye-sensitized solar cells with high efficiency. *Adv. Mater.* **2014**, *26*, 6210–6237. [CrossRef]

72. Zambrzycki, M.; Piech, R.; Raga, S.R.; Lira-Cantu, M.; Fraczek-Szczypta, A. Hierarchical carbon nanofibers/carbon nanotubes/NiCo nanocomposites as novel highly effective counter electrode for dye-sensitized solar cells: A structure-electrocatalytic activity relationship study. *Carbon* **2022**, *203*, 97–110. [CrossRef]

73. Cruz-Gutiérrez, C.A.; Félix-Navarro, R.M.; Calva-Yañez, J.C.; Silva-Carrillo, C.; Lin-Ho, S.W.; Reynoso-Soto, E.A. Carbon nanotube-carbon black hybrid counter electrodes for dye-sensitized solar cells and the effect on charge transfer kinetics. *J. Solid State Electrochem.* **2021**, *25*, 1479–1489. [CrossRef]

74. Brennan, L.J.; Byrne, M.T.; Bari, M.; Gun'ko, Y.K. Carbon nanomaterials for dye-sensitized solar cell applications: A bright future. *Adv. Ener. Mater.* **2011**, *1*, 472–485. [CrossRef]

75. Lee, C.-P.; Lin, C.-A.; Wei, T.-C.; Tsai, M.-L.; Meng, Y.; Li, C.-T.; Ho, K.-C.; Wu, C.-I.; Lau, S.-P.; He, J.-H. Economical low-light photovoltaics by using the Pt-free dye-sensitized solar cell with graphene dot/PEDOT: PSS counter electrodes. *Nano Energy* **2015**, *18*, 109–117. [CrossRef]

76. Kuppu, S.V.; Senthilkumaran, M.; Sethuraman, V.; Balaji, M.; Saravanan, C.; Ahmed, N.; Mohandoss, S.; Lee, Y.R.; Anandharaj, J.; Stalin, T. The surfactants mediated electropolymerized poly (aniline)(PANI)-reduced graphene oxide (rGO) composite counter electrode for dye-sensitized solar cell. *J. Phys. Chem. Solids* **2022**, *173*, 111121. [CrossRef]

77. Rafique, S.; Rashid, I.; Sharif, R. Cost effective dye sensitized solar cell based on novel Cu polypyrrole multiwall carbon nanotubes nanocomposites counter electrode. *Sci. Rep.* **2021**, *11*, 14830. [CrossRef]

78. Shih, Y.-C.; Lin, H.-L.; Lin, K.-F. Electropolymerized polyaniline/graphene nanoplatelet/multi-walled carbon nanotube composites as counter electrodes for high performance dye-sensitized solar cells. *J. Electroanal. Chem.* **2017**, *794*, 112–119. [CrossRef]

79. Reza, M.; Utami, A.N.; Amalina, A.N.; Benu, D.P.; Fatya, A.I.; Agusta, M.K.; Yuliarto, B.; Kaneti, Y.V.; Ide, Y.; Yamauchi, Y. Significant role of thorny surface morphology of polyaniline on adsorption of triiodide ions towards counter electrode in dye-sensitized solar cells. *New J. Chem.* **2021**, *45*, 5958–5970. [CrossRef]

80. Huang, K.-C.; Huang, J.-H.; Wu, C.-H.; Liu, C.-Y.; Chen, H.-W.; Chu, C.-W.; Lin, C.-L.; Ho, K.-C. Nanographite/polyaniline composite films as the counter electrodes for dye-sensitized solar cells. *J. Mater. Chem.* **2011**, *21*, 10384–10389. [CrossRef]

81. Yue, G.; Zhang, X.A.; Wang, L.; Tan, F.; Wu, J.; Jiang, Q.; Lin, J.; Huang, M.; Lan, Z. Highly efficient and stable dye-sensitized solar cells based on nanographite/polypyrrole counter electrode. *Electrochim. Acta* **2014**, *129*, 229–236. [CrossRef]

82. Chen, D.; Pei, Q. Electronic muscles and skins: A review of soft sensors and actuators. *Chem. Rev.* **2017**, *117*, 11239–11268. [CrossRef]

83. Jang, Y.; Kim, S.M.; Spinks, G.M.; Kim, S.J. Carbon nanotube yarn for fiber-shaped electrical sensors, actuators, and energy storage for smart systems. *Adv. Mater.* **2020**, *32*, 1902670. [CrossRef]

84. Zhang, S.; Zhang, H.; Cheng, J.; Zhang, W.; Cao, G.; Zhao, H.; Yang, Y. Novel polymer-graphite composite grid as a negative current collector for lead-acid batteries. *J. Power Source* **2016**, *334*, 31–38. [CrossRef]

85. Kumar, V.; Kumar, A.; Han, S.S.; Park, S.-S. RTV silicone rubber composites reinforced with carbon nanotubes, titanium-di-oxide and their hybrid: Mechanical and piezoelectric actuation performance. *Nano Mater. Sci.* **2021**, *3*, 233–240. [CrossRef]

86. Kumar, V.; Lee, G.; Choi, J.; Lee, D.-J. Studies on composites based on HTV and RTV silicone rubber and carbon nanotubes for sensors and actuators. *Polymer* **2020**, *190*, 122221. [CrossRef]

87. Costa, P.; Nunes-Pereira, J.; Oliveira, J.; Silva, J.; Moreira, J.A.; Carabineiro, S.; Buijnsters, J.; Lanceros-Mendez, S. High-performance graphene-based carbon nanofiller/polymer composites for piezoresistive sensor applications. *Compos. Sci. Technol.* **2017**, *153*, 241–252. [CrossRef]

88. Wei, X.-F.; Liu, J.-X.; Bao, W.; Qin, Y.; Li, F.; Liang, Y.; Xu, F.; Zhang, G.-J. High-entropy carbide ceramics with refined microstructure and enhanced thermal conductivity by the addition of graphite. *J. Eur. Ceram. Soc.* **2021**, *41*, 4747–4754. [CrossRef]

89. Irani, F.S.; Shafaghi, A.H.; Tasdelen, M.C.; Delipinar, T.; Kaya, C.E.; Yapici, G.G.; Yapici, M.K. Graphene as a Piezoresistive Material in Strain Sensing Applications. *Micromachines* **2022**, *13*, 119. [CrossRef]

90. Breen, M.S.; Long, T.C.; Schultz, B.D.; Williams, R.W.; Richmond-Bryant, J.; Breen, M.; Langstaff, J.E.; Devlin, R.B.; Schneider, A.; Burke, J.M. Air pollution exposure model for individuals (EMI) in health studies: Evaluation for ambient PM2. 5 in Central North Carolina. *Environ. Sci. Technol.* **2015**, *49*, 14184–14194. [CrossRef]

91. Chen, Y.; Yang, Y.; Xiong, Y.; Zhang, L.; Xu, W.; Duan, G.; Mei, C.; Jiang, S.; Rui, Z.; Zhang, K. Porous aerogel and sponge composites: Assisted by novel nanomaterials for electromagnetic interference shielding. *Nano Today* **2021**, *38*, 101204. [CrossRef]

92. Cao, M.-S.; Wang, X.-X.; Cao, W.-Q.; Yuan, J. Ultrathin graphene: Electrical properties and highly efficient electromagnetic interference shielding. *J. Mater. Chem. C* **2015**, *3*, 6589–6599. [CrossRef]

93. Wang, H.; Li, S.; Liu, M.; Li, J.; Zhou, X. Review on shielding mechanism and structural design of electromagnetic interference shielding composites. *Macromolecul. Mater. Eng.* **2021**, *306*, 2100032. [CrossRef]

94. Chung, D. Materials for electromagnetic interference shielding. *Mater. Chem. Phys.* **2020**, *255*, 123587. [CrossRef]

95. Yao, Y.; Jin, S.; Zou, H.; Li, L.; Ma, X.; Lv, G.; Gao, F.; Lv, X.; Shu, Q. Polymer-based lightweight materials for electromagnetic interference shielding: A review. *J. Mater. Sci.* **2021**, *56*, 6549–6580. [CrossRef]

96. Safdar, F.; Ashraf, M.; Javid, A.; Iqbal, K. Polymeric textile-based electromagnetic interference shielding materials, their synthesis, mechanism and applications—A review. *J. Ind. Text.* **2022**, *51*, 7293S–7358S. [CrossRef]

97. Thomassin, J.-M.; Jerome, C.; Pardoen, T.; Bailly, C.; Huynen, I.; Detrembleur, C. Polymer/carbon based composites as electromagnetic interference (EMI) shielding materials. *Mater. Sci. Eng. R Rep.* **2013**, *74*, 211–232. [CrossRef]

98. Zhang, W.; Wei, L.; Ma, Z.; Fan, Q.; Ma, J. Advances in waterborne polymer/carbon material composites for electromagnetic interference shielding. *Carbon* **2021**, *177*, 412–426. [CrossRef]

99. Shakir, M.F.; Khan, A.N.; Khan, R.; Javed, S.; Tariq, A.; Azeem, M.; Riaz, A.; Shafqat, A.; Cheema, H.M.; Akram, M.A. EMI shielding properties of polymer blends with inclusion of graphene nano platelets. *Res. Phys.* **2019**, *14*, 102365. [CrossRef]

100. Jeddi, J.; Katbab, A.A. AC electrical conductivity, shielding effectiveness and viscoelastic characteristics of nanocomposites based on RTV silicon rubber and nano graphite sheets/carbon black hybrid system. *AIP Conf. Proc.* **2017**, *1914*, 030013.

101. Jeddi, J.; Katbab, A.A.; Mehranvari, M. Investigation of microstructure, electrical behavior, and EMI shielding effectiveness of silicone rubber/carbon black/nanographite hybrid composites. *Polym. Compos.* **2019**, *40*, 4056–4066. [CrossRef]